IET Radar, Sonar & Navigation

Research Article

IET Journals
The Institution of Engineering and Technology

Good practical continuous waveform for active bistatic radar

ISSN 1751-8784
Received on 28th July 2015
Revised on 16th September 2015
Accepted on 29th September 2015
doi: 10.1049/iet-rsn.2015.0413
www.ietdl.org

Itzik Cohen[1], *Rafael Elster*[2], *Nadav Levanon*[1] ✉

[1]*Electrical Engineering – Systems, Tel-Aviv University, Tel-Aviv, Israel*
[2]*Elisra, Elbit Systems, Bnei Brak, Israel*
✉ *E-mail: nadav@eng.tau.ac.il*

Abstract: In monostatic continuous wave (CW) radar the dominant waveform is periodic linear frequency modulation, mostly because its stretch processing requires sampling rate much lower than the bandwidth. In a bistatic scene a clean copy of the transmitted signal, required in stretch processing, is not available to the receiver. That opens the competition for other periodic waveforms. The authors study describes and demonstrates, through bistatic field trials, the good performances of bi-phase and tri-phase CW waveforms. Among their advantages are sidelobe-free range response, availability at all prime lengths and ease of synchronisation. Successful bistatic operation is a prerequisite for multistatic systems.

1 Introduction

The prevailing waveform in continuous wave (CW) radar is periodic linear frequency modulation (LFM). LFM is popular mostly because it lends itself to simple stretch processing [1, 2]. Within the radar a low-power portion of the transmitted signal is diverted to the receiver where it is mixed with the delayed target return signal. A typical target delay is usually much shorter than the modulation period; hence, the mixer beat frequency is much lower than the sweep frequency span ($\simeq$ bandwidth). The low beat frequency allows low sampling rate, which simplifies the digital processor. In other aspects LFM is not such a good periodic signal. For example, its periodic auto-correlation (PAC) is not sidelobe-free, a property that several other periodic waveforms have. Intra-period weighting needs to be added in the LFM receiver to reduce range sidelobes, resulting signal-to-noise ratio (SNR) loss.

In bistatic (or multistatic) radar, the remote receiver does not have an exact, noise-free replica of the transmitted signal, hence the main advantage of LFM – simple stretch processing, is not easily recovered. Even after giving up on stretch processing, estimating the exact signal's parameters from the delayed, noisy, clutter embedded, direct reception, is more complicated than estimating the parameters of some of the other periodic waveforms. Furthermore, in multistatic radar it is important to have available a large family of member signals that can be well separated. LFM is not a good base for such a family, unless additional coding is overlaid on it.

Other potential CW radar waveforms are based on phase-coded pseudo-random sequences. Antipodal bi-phase values $\{+1, -1\}$ were proposed in [3] and discussed in [4–6]. Non-antipodal $\{+1, \exp(\mathrm{j}\phi)\}$ were proposed in [7].

Our paper presents two versions of a good CW waveform based on the non-antipodal bi-phase coding, because: (a) it produces sidelobe-free delay response, (b) its delay-Doppler response does not exhibit strong recurrent peaks in Doppler and (c) its parameters can be estimated relatively easily by a cooperative bistatic receiver, which has prior knowledge of the code and of the specified code-element duration. One version of the signal exhibits very low spectral sidelobes that allow lower sampling frequency than what conventional phase-coded waveforms require. Finally, the proposed waveform offers many separable signals belonging to the same family.

Experimental results are presented and practical issues of bistatic processing are discussed. The experiments emphasised detection of slow moving targets in stationary clutter.

2 Proposed CW waveform

The proposed waveform is based on m-sequences [8] or Legendre sequences [9], modified [9–11] such that the binary values $\{+1, -1\}$ are replaced by $\{+1, \exp(\mathrm{j}\phi)\}$ correspondingly, where [11]

$$\phi = \cos^{-1}\left(-\frac{N-1}{N+1}\right) \tag{1}$$

and N is the sequence length. Modern waveform generators can generate such non-antipodal two-valued alphabet. In the following sections we will compare the performances of the proposed signal against LFM. The LFM time-bandwidth (TBW) product will be identical to the sequence length, thus yielding the same compression ratio.

2.1 Comparing periodic ambiguity functions

The comparison will be based on the periodic ambiguity function (PAF) [12]. PAF describes the performances of a specific coherent processor based on cross-correlation between the received signal and an integer (P) number of periods of the noise-free signal. Such a processor optimises SNR, while P affects the Doppler resolution. Doppler and range sidelobes can be reduced by adding weight window to the reference. In that case the proper name of the resulted response is the periodic cross-ambiguity function (PCAF).

Bi-phase periodic waveforms exhibit two major properties that periodic LFM does not have: (a) perfect PAC, (b) PAF with a low recurrent ridge at Doppler values equal to the inverse of the waveform period. The different properties of the two signals are demonstrated in Figs. 1 and 2, which display the PCAF of LFM and bi-phase waveforms with compression of 1023.

The term PCAF is used to describe the plots because the receivers use inter-period Hamming weighted reference in order to lower the Doppler sidelobes. To obtain a readable drawing, we selected $P = 64$. In the field experiments we used $P = 2048$. The vertical scale of both drawings is in decibels (dB). The total duration of the bi-phase reference signal was $PT_r = PNt_b = Mt_b$, where t_b is the duration of a phase element (bit) and T_r is the period. The LFM signal has the same period T_r and its reference contains the same number of periods $P = 64$.

To demonstrate that both signals have the same compression (delay resolution), Figs. 3 and 4 zoom on the delay scale, showing only ±2% of one period. They both show a first delay null at about $T_r/1023$.

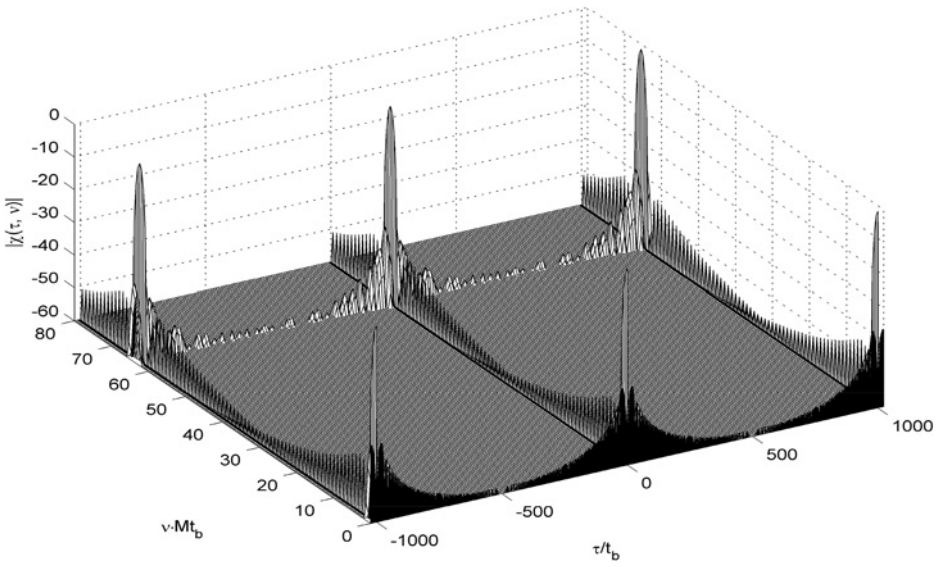

Fig. 1 *PCAF (in dB) of LFM waveform with Hamming weighted reference of 64 periods*

There are two basic differences between the PCAFs: (a) LFM exhibits sidelobes along the delay axis, while bi-phase is sidelobe-free, (b) at Doppler ν equal to the inverse of the period $\nu = 1/T_r$ or $\nu M t_b = P$, LFM exhibits recurrent periodic peaks almost identical to the periodic peaks at zero Doppler. These recurrent peaks will maintain their full height – slightly lower than 1 (≃0 dB), no matter how much the TBW is increased. On the other hand, the bi-phase waveform exhibits a low ridge whose height is approximately equal to the inverse of the square root of the sequence length: namely

$$\left|\chi\left(\tau,\ 1/T_r\right)\right| \simeq 1/\sqrt{N} \tag{2}$$

With $N = 1023$, which is the case in Figs. 2 and 4, the ridge height is ∼0.03 or −30 dB. Doubling the code length ($N = 2047$) will lower the ridge height to −33 dB, and so on.

It should be noted that in LFM, adding intra-period amplitude weighting to the reference signal can reduce the sidelobes along the delay axis. One penalty is widening of the mainlobe. This is demonstrated in Fig. 5, where Hamming intra-period weighting was added. Another penalty is an additional SNR loss of ∼1.5 dB. Comparing Fig. 5 with Fig. 4 shows that bi-phase coding still maintains an edge over LFM, with regard to the PCAF.

2.2 Comparing spectrums

One advantage of LFM is its spectral efficiency. Its spectrum is relatively flat and drops rather rapidly out of band (Fig. 6, top). In contrast, the bi-phase waveform exhibits relatively high out-of-band spectral sidelobes (Fig. 6, middle). In addition to possible interference to spectral neighbours, the sidelobes of the bi-phase waveform imply that the receiver has to sample the signal at a rate corresponding to the wider bandwidth (including the significant sidelobes), if the signal properties (e.g. perfect PAC) are to be maintained. Initial experiments hinted that at least 8 samples/bit are necessary. Spectral sidelobe reduction of phase-modulated radar waveforms received recent attention because of European Telecommunications Standards Institute (ETSI) regulations regarding automotive radar [13].

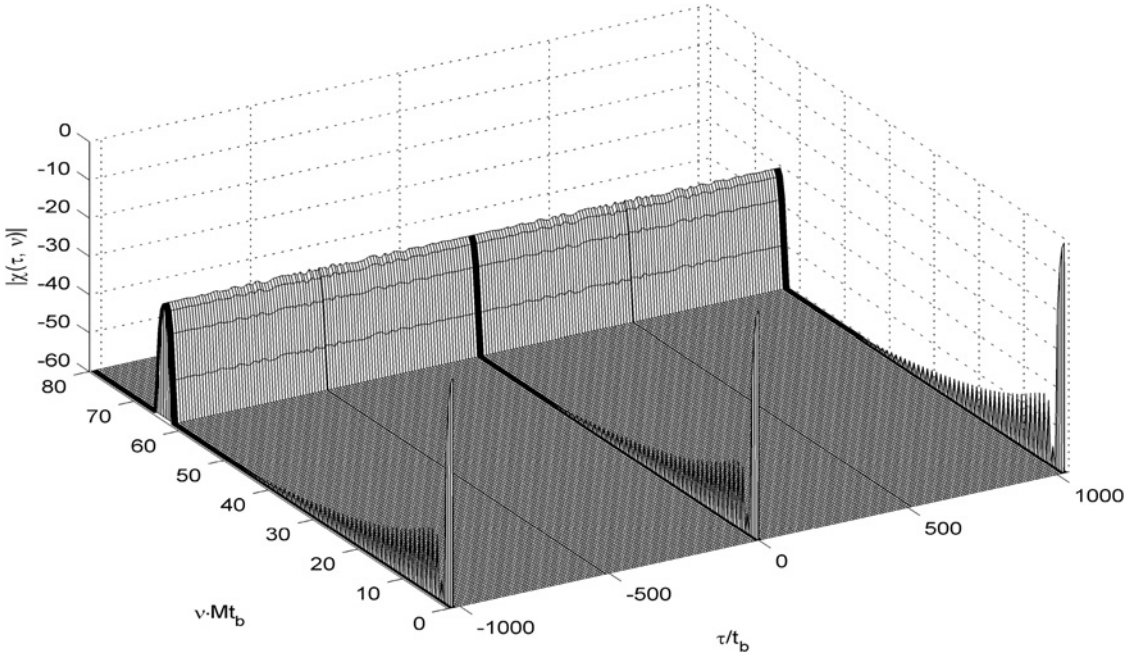

Fig. 2 *PCAF (in dB) of bi-phase waveform with Hamming weighted reference of 64 periods*

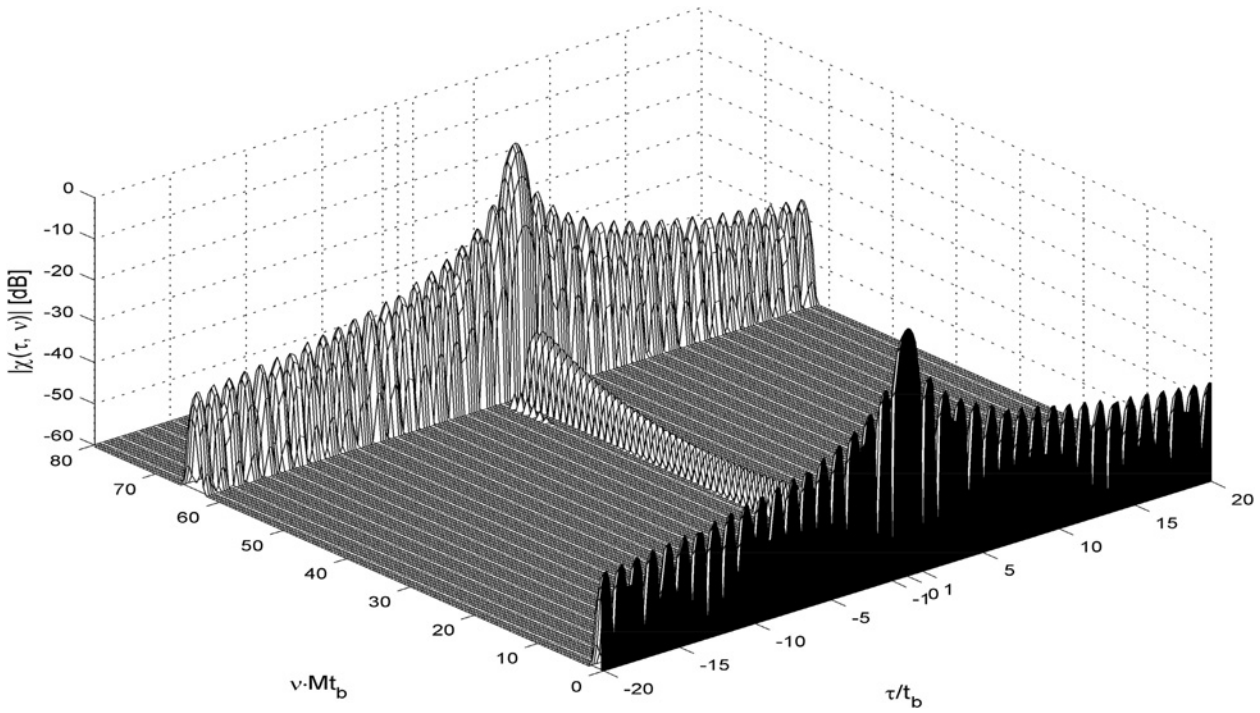

Fig. 3 *Zoom on the PCAF of the LFM waveform*

We suggest a second version of the bi-phase waveform that exhibits more efficient spectrum, with negligible spectral sidelobes. In that version the rectangular shape of a bit is replaced by a 'Gaussian-weighted sinc' (GWS) [14]

$$\mathrm{GWS}_m = \exp\left[-\frac{1}{2}\left(\frac{4m}{\sigma(4M+1)}\right)^2\right]\frac{\sin\,\alpha_m}{\alpha_m},$$
$$\alpha_m = \frac{4\pi m}{4M+1},\ m = -2M,\ -2M+1,\ \ldots,\ 2M \qquad (3)$$

where M is the number of samples per code element (bit) and σ is a parameter chosen as 0.7. Fig. 7 shows the shape of a bit when $M = 4$. The shape extends over the length of four rectangular bits, and includes polarity reversals. The spectrally efficient waveform is created by convolving the GWS with the non-antipodal waveform. Using bi-phase waveform with the modified bit shape creates amplitude variations. Fig. 8 shows a section of the modified bi-phase waveform, based on 103 elements Legendre code. A linear power radio frequency (RF) amplifier is required in order to faithfully transmit such a signal. This is not a major obstacle because

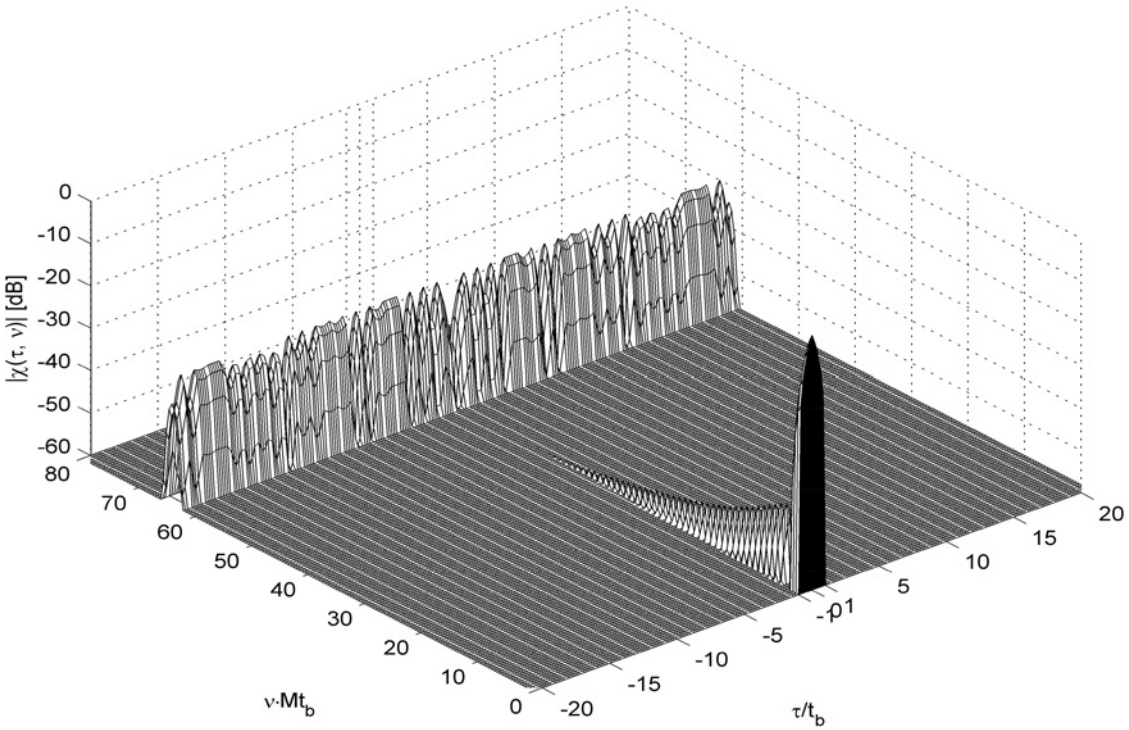

Fig. 4 *Zoom on the PCAF of the bi-phase waveform*

IET Radar Sonar Navig., 2016, Vol. 10, Iss. 4, pp. 798–806

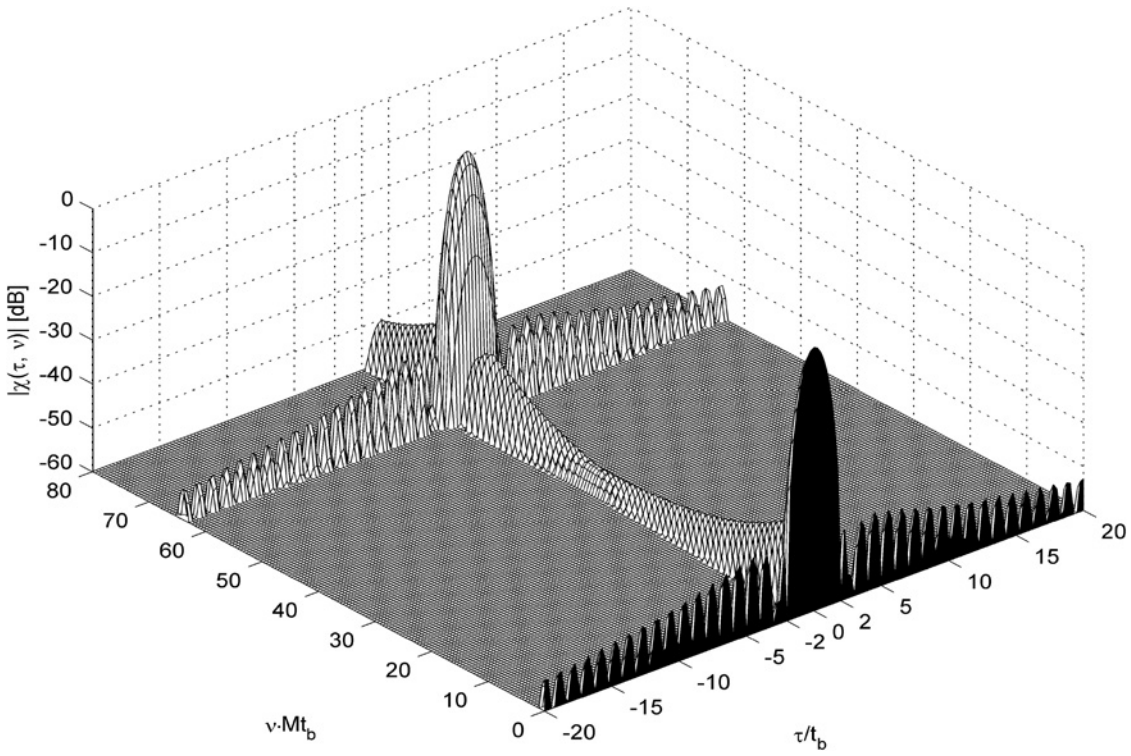

Fig. 5 *Zoom on the PCAF of the LFM waveform. Hamming intra-period added to the reference*

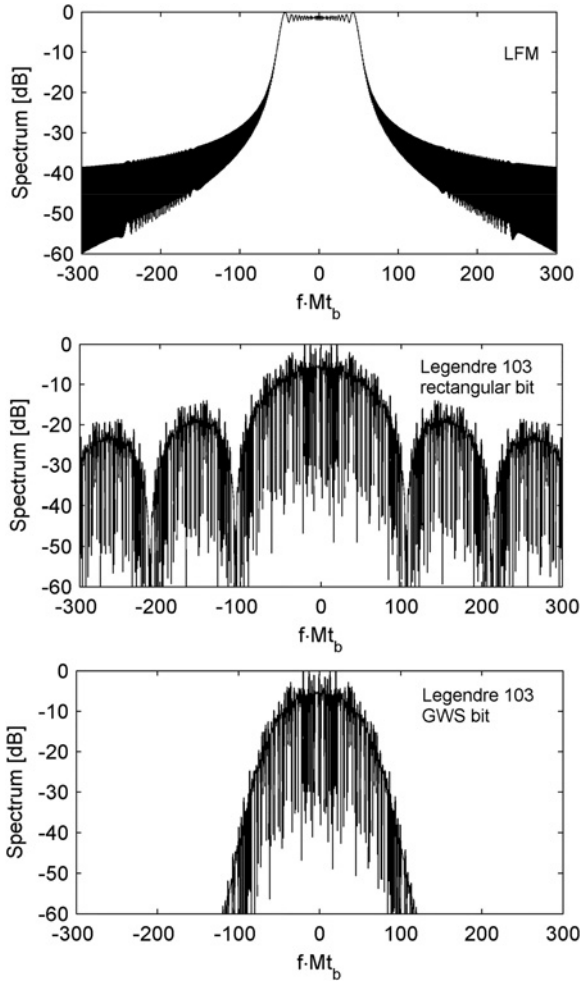

Fig. 6 *Spectrums of waveform with 103 compression factor: LFM (top), Legendre with rectangular bit (middle) and Legendre with GWS using 4 samples/bit (bottom)*

CW signals require relatively low peak power. Furthermore, as Fig. 8 (top subplot) shows, the peak-to-mean envelope ratio is close to one.

The resulted spectrum of the modified signal is shown in Fig. 6 (bottom), which should be compared with the original spectrum (Fig. 6, middle). Initial experiments with GWS waveform suggest that 4 samples/bit are sufficient to maintain the perfect PAC property.

In summary, the original version of the bi-phase waveform can use non-linear RF power amplifiers in the transmitter, but requires 8 samples/bit on receive, and exhibits inefficient spectral usage. The modified GWS version use the spectrum efficiently, needs only 4 samples/bit on receive, but requires linear power amplifiers in the transmitter.

3 Signals availability and separability

A binary phase shift keying code of length N that can be modified according to (1) to yield a sequence with perfect PAC must correspond to a 'cyclic difference set' [11, 15]. The available sequence lengths N are determined by the type of difference set as listed in Table 1. The combination of the lengths of Legendre and Legendre (3 phase) sequences cover all the prime numbers (excluding 2).

Legendre sequences provide the majority of available lengths N, but at each length there is only one unique sequence. The term unique implies that permutations such as left-right flips or phase interchanges are not counted. '*m*-sequences' are available at fewer lengths N, but there are many unique codes at each length. As an example, a list of available codes for $899 \leq N \leq 1091$ is listed in Table 2.

In multistatic radar systems several radar transmitters operate simultaneously, each using its unique code. Knowing the codes, a receiver is expected to receive several transmissions and separate them. Especially good separation between a pair of signals is obtained from two sequences of near but different lengths, when the number of coherently processed periods is large. Table 3 presents the peak cross-correlation when a receiver matched to P periods of periodic sequence of length $N_1 = 1023$ receives a CW periodic signal coded by a sequence of length $N_2 = 1019$. According to Table 3 processing coherently a large number (P) of periods improves the separability between different waveforms from the same family. This agrees well with the fact that large P

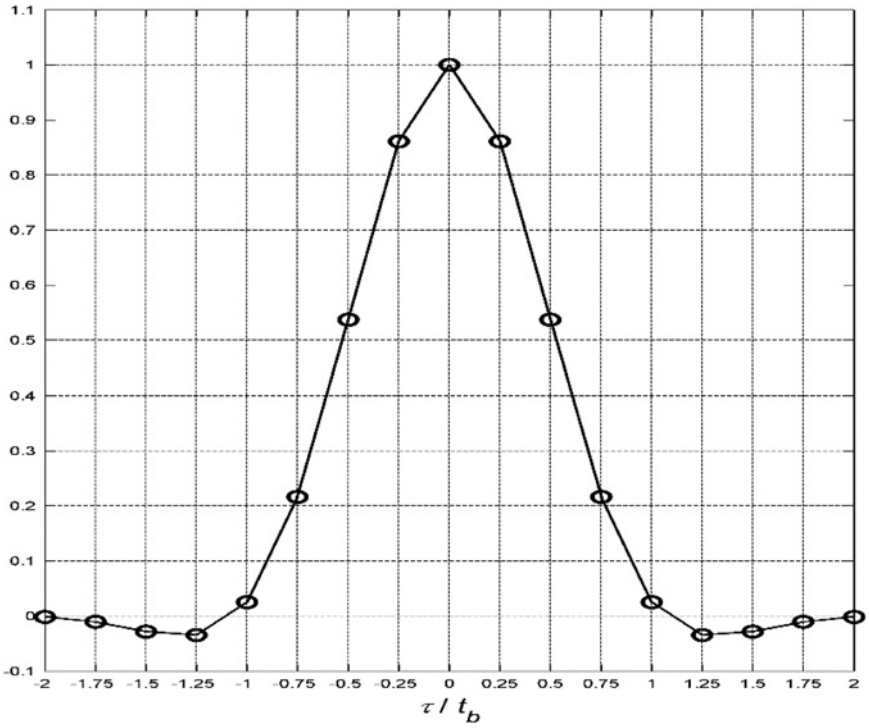

Fig. 7 *GWS with 4 samples/bit*

improves the Doppler resolution. In the experiments we used $P = 2048$, which provided a target velocity resolution of 0.32 m/s that helps to observe slow moving targets.

3.1 Legendre (3 phase)

A sub-family of the Legendre sequences is available for sequence lengths $N = 4m-3$, when N is a prime and m is a positive integer [16]. It differs from the original sequence family, in which $N = 4m-1$, by using three complex values: $\{1, \exp(j\alpha), \exp(j\alpha/2)\}$. The third value appears only once, in the first element of the sequence. The Appendix shows MATLAB construction of such a code, as well as the 2-phase code.

4 Bistatic and multistatic receiver considerations

The physical separation between the receiver and the transmitter makes it very complicated to have a common reference clock. Therefore, the receiver cannot use for reference signal the exact

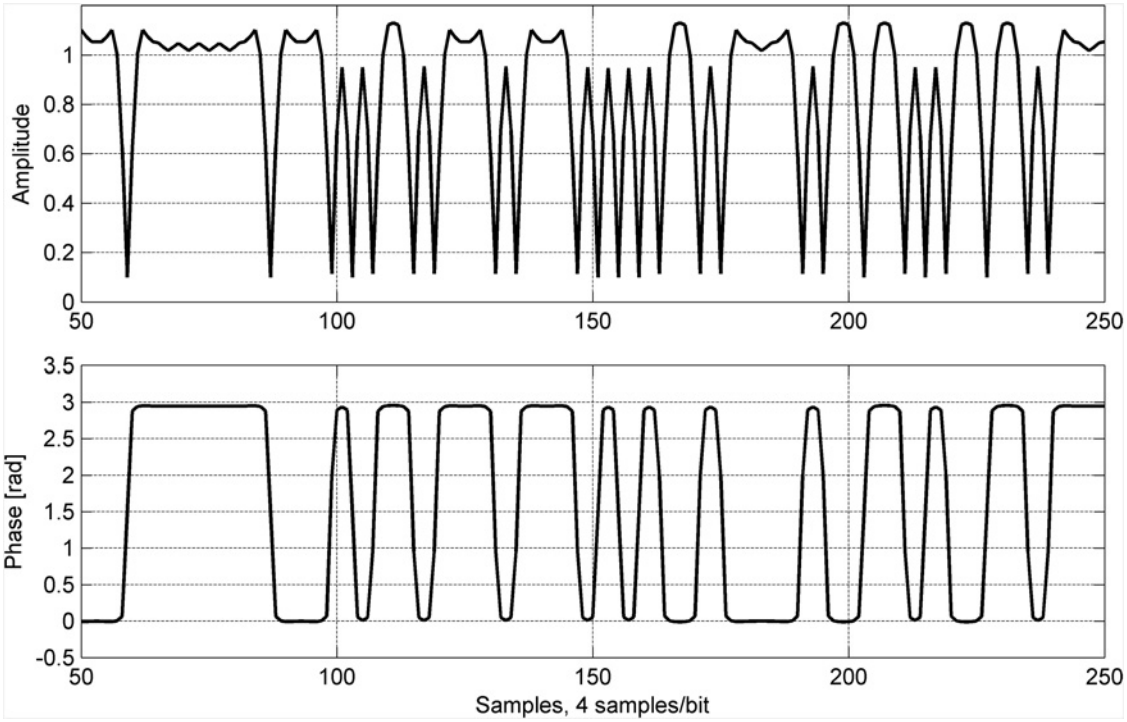

Fig. 8 *Section (≃50 bit) from a bi-phase 103 element Legendre code utilising bits shaped as GWS with 4 samples/bit*

IET Radar Sonar Navig., 2016, Vol. 10, Iss. 4, pp. 798–806

Table 1 Types of suitable difference sets

N	Restrictions	Type
$N=2^m-1$	m positive integer	m-sequence over GF(2^m)
$N=4m-1$	N is prime, m is positive integer	Legendre or quadratic residue
$N=4m-3$	N is prime, m is positive integer	Legendre (three phase)
$N=4m^2+27$	m positive integer	Hall's sextic residue
$N=p(p+2)$	p and $(p+2)$ are primes	twin primes

waveform the transmitter uses. What is practical to assume is that the receiver knows exactly the code sequence, code length and bit shape, and have some coarse quantitative knowledge of the bit rate and carrier frequency. To reach synchronisation, the receiver needs to estimate the exact bit rate, carrier frequency and the in-period phase (the zero delay) [17].

The synchronisation can be performed by locking both receiver and transmitter on a common reference signal, for example, by using a global positioning system (GPS) receiver as a common reference source [18, 19]. Another approach is direct synchronisation [20], where the receiver intercepts the transmitted signal through the direct transmitter–receiver path and demodulates it by passing the signal through its nominal matched filter. An error in the assumed carrier frequency is expressed as a Doppler shift of the stationary direct reception. An error in the bit rate is expressed as a drift in the delay of the direct path reception. If there is no line of sight between the transmitter and the receiver, the process can be performed using a reflection through a known stationary scatterer. The following experiments did not include instrumentations for GPS-aided synchronisation and the synchronisation was performed through direct reception. The synchronisation process itself was performed much like the synchronisation process in spread-spectrum communication systems [21, 22], with emphasis on synchronisation under heavy multipath environment [23]. In a bistatic case, stretched processing

Table 2 Codes availability for $899 \leq N \leq 1091$

Length N	Number of unique codes	Type
899	1	twin primes (29 and 31)
907	1	Legendre
911	1	Legendre
919	1	Legendre
927	1	Hall's sextic residue
929	1	Legendre (three phase)
937	1	Legendre (three phase)
941	1	Legendre (three phase)
947	1	Legendre
953	1	Legendre (three phase)
967	1	Legendre
971	1	Legendre
977	1	Legendre (three phase)
983	1	Legendre
991	1	Legendre
997	1	Legendre (three phase)
1009	1	Legendre (three phase)
1013	1	Legendre (three phase)
1019	1	Legendre
1021	1	Legendre (three phase)
1023	60	m-sequence
1031	1	Legendre
1033	1	Legendre (three phase)
1039	1	Legendre
1049	1	Legendre (three phase)
1051	1, 1	Legendre, Hall's sextic residue
1061	1	Legendre (three phase)
1063	1	Legendre
1069	1	Legendre (three phase)
1087	1	Legendre
1091	1	Legendre

Table 3 Cross-correlation between sequences of lengths 1023 and 1019

P (number of periods processed coherently)	1	4	16	64	256	1024
cross-correlation peak value, dB	−19.8	−26.3	−32.4	−40.5	−46.9	−59.4

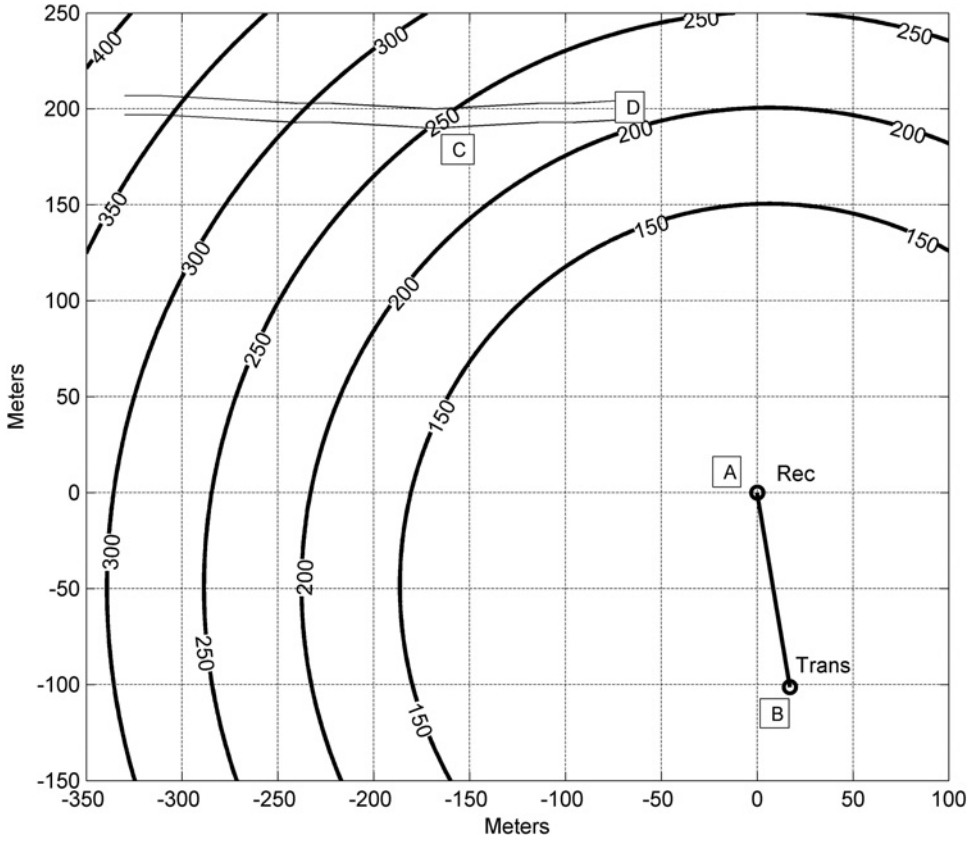

Fig. 9 *Bistatic field trial*

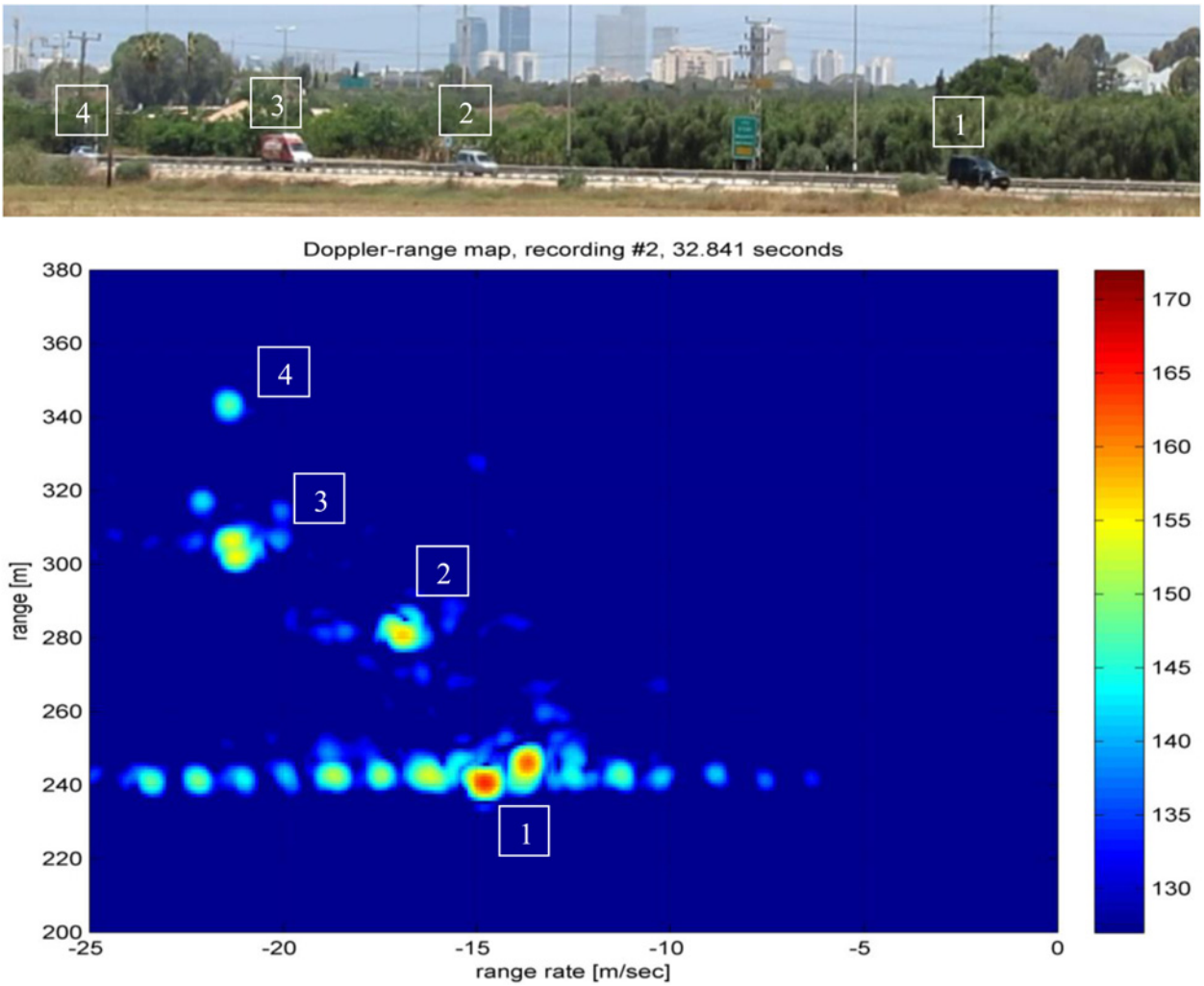

Fig. 10 *Road scene with four approaching cars and the corresponding range/range-rate radar display. Outside guard-rail ends just behind the closest car (#1, black). The colour bar is in dB*

of an LFM waveform is relatively complicated, as the receiver requires a synchronised analogue replica of the LFM signal. Hence the main advantage of LFM and stretched processing – simplicity, is partially lost. This drawback intensifies for the multistatic case, as a synchronised analogue replica is required for each of the transmitted LFM signals.

5 Experimental results

Several field trials were conducted with a low-power (1 W) CW radar using the phase-coded waveform. The first (out of two) to be described is a fully bistatic trial, conducted in June 2014. The signal parameters were:

(i) *Code:* 1023 element modified *m*-sequence.
(ii) *Element width:* 25 ns (3.75 m range resolution) → spectral width: 40 MHz.
(iii) *Element representation:* GWS (Fig. 7).
(iv) Four samples/element (sampling rate = 160 MHz, off-line processing).
(v) *Maximum unambiguous range:* 3836 m (=1023 × 3.75).
(vi) Number of periods processed coherently: 2048.
(vii) Total coherent processing interval (CPI): 52.4 ms (=25 ns × 1023 × 2048).
(viii) Doppler resolution (1/CPI): 19 Hz.
(ix) Velocity resolution (at 9 GHz carrier frequency): 0.32 m/s (=1.14 km/h).
(x) Maximum unambiguous velocity: ±326 m/s.

The geographic outline is shown in Fig. 9. The transmitter was located at point B and the receiver at point A. The baseline length

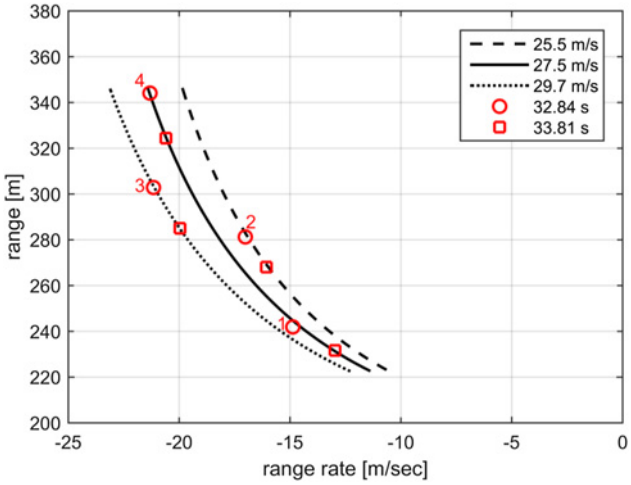

Fig. 11 *Expected road speeds of the cars in Fig. 10*

IET Radar Sonar Navig., 2016, Vol. 10, Iss. 4, pp. 798–806

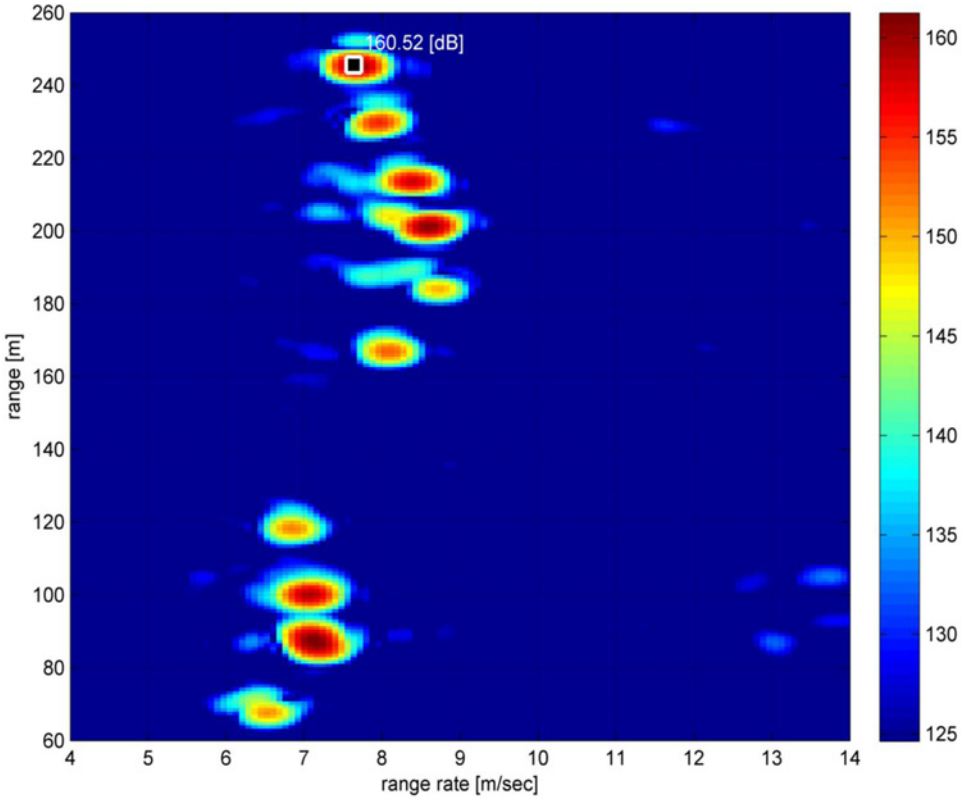

Fig. 12 *Ten receding cars (colour bar in dB)*

$\overline{AB} = b \simeq 100$ m. The contour lines represent

$$\text{contour value} = \frac{1}{2}\left(R_{\text{target}-\text{trans}} + R_{\text{target}-\text{rec}} - b\right) \tag{4}$$

The targets were cars travelling on a road, a section of which is marked by the two thin lines on both sides of $y = 200$ m. There were guard-rails between the approaching and receding lanes (two lanes in each direction). There was also a guard-rail on the road edge facing the radar, except for section CD. To demonstrate the resolutions and dynamic range of the radar we picked a scene (Fig. 10, top) photographed from the receiver location, showing four approaching cars. The corresponding delay/Doppler (range/range-rate) radar display appears in Fig. 10 (bottom). Note that the wheels of three cars are obscured because of the guard-rail. Only the closest car (#1, black) is in full view. The radar display of the closest car is dramatically different from the other cars. It includes widely stretching micro-Doppler returns contributed by the visible car wheels. It is intuitively clear that if a car moves along the road with velocity of V_{car} the lowest section of the wheel has zero forward velocity (the wheel does not slip on the road), while the forward speed of the top section of the wheel is $2V_{\text{car}}$. The forward velocities of other sections of the wheel are distributed between these values. Indeed the Doppler spread of the closest target is to the right and left of the strong main scattering of the car's body. Since the lower half of a wheel is less visible to the radar, the low velocity micro-Dopplers decay faster than the high velocity ones.

Knowing the road track in addition to the transmitter and receiver locations makes it possible to estimate the true car velocities from a single radar snapshot. Assuming that the four cars were moving along the line $y = 200$ in Fig. 9, yields the expected range-rate evolution shown in Fig. 11. The drawing displays range versus range-rate for different velocities, overlaid by the corresponding coordinates of the four cars (circles), obtained from the lower half of Fig. 10. The resulted velocities are 92, 99 and 107 km/h. These are expected road velocities (the speed limit is 90 km/h). The four range/range-rate coordinates marked by the numbered squares were obtained from a subsequent radar snapshot, taken one second later.

A second trial (March 2013) was bistatic in the electrical sense, but the transmitter and the receiver were co-located on the roof of a four story building looking downward on a narrow one-way ally. The delay-Doppler plot (Fig. 12) shows ten cars driving away slowly. Note the complete lack of range sidelobes due to the perfect periodic cross-correlation of the waveform. The almost sidelobe-free Doppler response is due to a unique weight window [24] that preceded the processor's fast Fourier transform (FFT). Some cars display wheels micro-Doppler at lower velocity than the cars'. This is attributed to the fact that the radar was viewing the cars from above, giving better exposure to the lower (and slower) parts of the wheels. Fig. 12 demonstrates also the wide dynamic span between car returns ($\simeq$160 dB) and the background ($\simeq$125 dB).

In both field trials the transmitted signal was generated by a vector signal generator (Agilent, E8267D), followed by a 1 W solid–state linear RF power amplifier. The received signal was down converted to base-band and synchronously sampled (Signatec, PDA-16) at a rate of 160 MS/s.

6 Conclusions

The suitability of bi-phase CW signals to bistatic radar is studied and demonstrated in field trials. In bistatic scenes, the relatively large distance between transmitter and receiver deprives the popular CW-LFM signal from its main advantage – simple stretch processing. Bi-phase coding can step in and provide sidelobe-free range response, low Doppler recurrent lobes and relative ease of transmitter–receiver synchronisation through direct reception. Spectral efficiency (low spectral sidelobes) is achieved by representing a code element (bit) by a 'GWS', stretching over 4 bits and using 4 samples/bit. The penalty is variable amplitude,

hence transmitter with linear RF power amplifier. Suitable families of periodic sequences were proposed and the expected separability between different signals was investigated for the sake of multistatic scenes.

7 References

1 Rohling, H., Kronauge, M.: 'Continuous waveforms for automotive radar systems', in Gini, F., DeMaio, A., Patton, L. (EDs.): 'Waveform design and diversity for advanced radar systems' (IET, London, 2012), pp. 173–205, Ch. 7
2 Keel, B.M., Baden, J.M.: 'Stretch processing', in Melvin, W.L., Scheer, J.A. (EDs.): 'Principles of modern radar – advanced techniques', (SciTech Publishing, Edison, NJ, 2013), pp. 26–40, Ch. 2.2
3 Albanese, D.F., Klein, A.M.: 'Pseudorandom code waveform design for CW radar', *IEEE Trans. Aerosp. Electron. Syst.*, 1979, **15**, (1), pp. 67–75
4 Olsen, K.E., Johnsen, T., Johnsrud, R., *et al.*: 'Results from an experimental continuous wave low probability of intercept bistatic radar – the first step toward multistatic radar'. Int. Radar Conf., 2003, pp. 288–292
5 Norland, R.: 'Digital signal processing in binary phase coded CW multistatic radar'. Int. Radar Conf., 2003, pp. 299–302
6 Johnsen, T., Olsen, K.E., Johnsrud, S., *et al.*: 'Simultaneous use of multiple pseudo random noise codes in multistatic CW radar'. IEEE Radar Conf., 2004, pp. 266–270
7 Levanon, N.: 'CW alternatives to the coherent pulse train signals and processors', *IEEE Trans. Aerosp. Electron. Syst.*, 1993, **29**, (1), pp. 250–254
8 Golomb, S.W.: 'Shift register sequences' (Aegean Park Press, Laguna Hills, CA, 1982, revised edn.)
9 Ipatov, V.P.: 'Spread spectrum and CDMA principles and applications' (Wiley, Chichester, England, 2005), Sec. 6.6–6.11
10 Amianatov, I.N.: 'Selected issues of statistical communications theory' (So. Radio, Moscow, 1971), pp. 334–337, (in Russian)
11 Golomb, S.W.: 'Two-valued sequences with perfect periodic autocorrelation', *IEEE Trans. Aerosp. Electron. Syst.*, 1992, **28**, (2), pp. 383–386
12 Levanon, N.: 'The periodic ambiguity function – its validity and value'. IEEE Int. Radar Conf., 2010, Washington, DC, USA, pp. 204–208
13 Giannini, V., Guemandi, D., Shi, Q., *et al.*: 'A 79 GHz phase-modulated 4 GHz-BW CW radar transmitter in 28 nm CMOS', *IEEE J. Solid-State Circuits*, 2014, **49**, (12), pp. 2925–2937
14 Chen, R., Cantrell, B.: 'Highly bandlimited radar signals'. IEEE Radar Conf., 2002, Long Beach, CA, pp. 220–226
15 Golomb, S.W., Gong, G.: 'Signal design for good correlation for wireless communication, cryptography, and radar' (Cambridge University Press, 2005)
16 Bomer, L., Antweiler, M.: 'Perfect three-level and three-phase sequences and arrays', *IEEE Trans. Inf. Theory*, 1994, **42**, (2,3,4), pp. 767–772
17 Willis, N.J.: 'Bistatic Radar' (Artech House, Boston, MA, 1991)
18 Wang, W.Q.: 'GPS-based time & phase synchronization processing for distributed SAR', *IEEE Trans. Aerosp. Electron. Syst.*, 2009, **45**, (3), pp. 1040–1051
19 Weiß, M.: 'Synchronization of bistatic radar systems'. IEEE Geoscience and Remote Sensing Symp., Anchorage, AK, 2004
20 Wang, W.Q.: 'Time and phase synchronisation via direct-path signal for bistatic synthetic aperture radar systems', *IET Radar Sonar Navig.*, 2008, **2**, (1), pp. 1–11
21 Proakis, J.: 'Digital communications' (McGraw-Hill, New York, 2000, 4th edn.)
22 Simon, M.K.: 'Spread spectrum communications handbook' (McGraw-Hill, New York, 2002)
23 Kaplan, E.D.: 'Understanding GPS: principles and applications' (Artech House, Norwood, MA, 2006, 2nd edn.)
24 Cohen, I., Levanon, N.: 'Weight windows – an improved approach'. 2014, IEEE 28th Convention of Electrical and Electronics Engineers in Israel, Eylat, Israel, 3–5 December 2014. Available at http://www.ieeexplore.ieee.org/stamp/stamp.jsp?tp=&arnumber=7005852

8 Appendix

MATLAB function for constructing a phase-coded periodic waveform of any odd-prime length, based on Legendre sequences. See Fig. 13.

```
function [ s ] = perfect_periodic_Legendre_waveform( N )
% Generates a periodic coded signal using 2 or 3 phases
% The signal exhibits perfect periodic autocorrelation
% N is any odd prime
Nspt=sprintf('%g element phase-coded waveform ',N);
if isprime(N)==0
    disp('Not a prime')
return
end
s=ones(1,N);
if rem((N+3)/4,1)==0
    c=0.25*(N-1);
    c1=2-1/c-1/(2*c^2);
    c2=1-1/c-1/(4*c^2);
    arg2=acos(-c1/2-sqrt((c1/2)^2-c2));
    s(mod((1:N-1).^2,N)+1)=exp(1i*arg2);
    s(1)=exp(1i*arg2/2);
else
    arg3=acos(-(N-1)/(N+1));
    s(mod((1:N-1).^2,N)+1)=exp(1i*arg3);
end
d=abs(ifft(fft(s).*conj(fft(s))));
figure, plot(d, 'k')
title(['Periodic autocorrelation of ' Nspt ]);
end
```

Fig. 13 *MATLAB function for constructing a phase-coded periodic waveform of any odd-prime length*